Inorganic Chemistry

Article

pubs.acs.org/IC

# Geometric Change of a Thiacalix[4]arene Supramolecular Gel with Volatile Gases and Its Chromogenic Detection for Rapid Analysis

Ka Young Kim,[†] Sunhong Park,[†] Sung Ho Jung,[†] Shim Sung Lee,[†] Ki-Min Park,[†] Seiji Shinkai,[‡] and Jong Hwa Jung*[,†]

[†]Department of Chemistry & Research Institute of Natural Science, Gyeongsang National University, Jinju 660-701, Republic of Korea

[‡]Faculty of Engineering, Sojo University, Komamoto 860-0082, Japan

Supporting Information

**ABSTRACT:** A coordination polymer gel that is self-assembled to form a network structure between a thiacalix[4]arene derivative (**L**) and $Co^{2+}$ has been prepared. This gel is capable of selectively changing color in the presence of gases that yield hydrogen chloride upon hydrolysis. The UV−vis absorption spectrum of a coordination polymer gel derived from $Co(NO_3)_2$ exhibits an absorption band at 527 nm and is colored red, indicating the formation of an octahedral $Co^{2+}$ complex. Treatment with a small amount of volatile gases containing a chlorine atom (VGCl) causes a red shift of ∼150 nm, resulting in a new strong band with a maximum at 670 nm and a color change to blue. In addition, the red color of the filter paper coated with a $Co(NO_3)_2$ coordination polymer gel changed to blue upon exposure to VGCl, reflecting a change in the coordination geometry. Red and blue colors of single crystals of $Co^{2+}$ complexes were obtained from a basic solution. From X-ray crystallographic analysis, the red $Co^{2+}$ complex corresponds to an octahedral structure, while the blue $Co^{2+}$ complex reflects the presence of a tetrahedral structure. Thus, the induced color change of $Co^{2+}$ gel from red to blue upon exposure to VGCl is due to the coordination geometry. The quantitative concentration of VGCl was calculated by employing the RGB histogram available in a smartphone application.

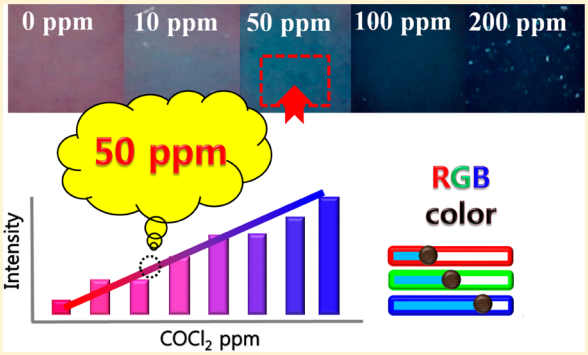


## INTRODUCTION

Recently, the design of supramolecular gels based on the concept of coordination polymers has attracted interest because of various potential applications that include gas storage, molecular sieves, ion exchange, sensing, and catalysis.[1−12] In particular, the photophysical properties of coordination polymer gels such as emission and absorption have been controlled with metal ions including alkali-earth and transition-metal ions.[13−18] Among these, $Co^{2+}$ coordination polymer gels have been demonstrated to exhibit thermochromic properties involving red or blue color changes with temperature that parallel the interchange between octahedral and tetrahedral structural forms. Indeed, such color changes for $Co^{2+}$ upon a change of the coordination geometry are often quite sensitive to the temperature, anion, and ligand concentration. For example, Kimizuka and co-workers[19] reported color changes for lipophilic $Co^{2+}$ triazole complexes in both gel and solution states whose reversibilities were temperature-dependent. These workers also reported that the blue color of the $Co^{2+}$ complex is due to the tetrahedral ($T_d$) structure in the gel state, whereas the red color of the $Co^{2+}$ complex corresponds to the octahedral ($O_h$) structure. Very recently, we have also discussed the color changes of the $Co^{2+}$ coordination polymer gel incorporating various anions.[20] However, there has been no previous study of the role of the coordination structure influencing the color changes of $Co^{2+}$ complexes with triazole- or tetrazole-based ligands. Although the coordination geometries of $Co^{2+}$ complexes with $O_h$, $T_d$, and mixed $T_d$−$O_h$ geometries in solution have been investigated by UV−vis absorption spectroscopy and by single-crystal X-ray crystallography,[21−27] the relationship between mixed geometries and the color of the $Co^{2+}$ complexes in supramolecular gels has not been reported. In view of this, we now report a systematic study of a $Co^{2+}$ coordination polymer gel based on the thiacalix[4]-arene framework and explore the concept of using the gasochromic property of this material as chemoprobes for volatile gases containing chlorine atom (VGCl) such as HCl, $SOCl_2$, $(COCl)_2$, and $COCl_2$.

Calix[4]arene-based ligands, a family of bowl-shaped polyphenol ligands with four hydroxyl groups at the lower rim, have been reported to be versatile candidates to construct polymeric network structures.[28−44] Since the replacement of the methylene linkages by sulfide groups, thiacalix[4]arenes have acquired various distinctive characteristics (more coordination sites, lower electron density, and more flexibility). One

**Received:** November 8, 2013
**Published:** February 24, 2014

   dx.doi.org/10.1021/ic402804p | *Inorg. Chem.* 2014, 53, 3004−3011

thiacalix[4]arene molecule can bind up to four metal ions simultaneously, forming a (metal)4-thiacalix[4]arene building block that can support various polymeric structures.[45−53] As a consequence, we chose thiacalix[4]arene as the framework for the attachment of ligands. In this paper, we describe the preparation of carboxylic acid-appended thiacalix[4]arene coordination polymer gels incorporating $Co^{2+}$. We also describe the color change that occurs with specific gases that liberate VGCl upon contact with the gas phase. The color changes of a $Co^{2+}$-induced gel by the introduction of VGCl in the isolated system were indirectly demonstrated by X-ray crystallographic analysis of the single crystals of $Co^{2+}$ complexes obtained in a hydrothermal reaction. Furthermore, we extended our studies to filter paper coated with a $Co^{2+}$ coordination polymer gel that successfully detected VGCl by the naked eye.

## EXPERIMENTAL SECTION

**General Considerations.** $^1H$ and $^{13}C$ NMR spectra were measured on a Bruker DRX 300 apparatus. IR spectra were obtained for KBr pellets, over the range 400−4000 $cm^{-1}$, with a Shimadzu FT-IR 8400S instrument, and mass spectra were obtained by a JEOL JMS-700 mass spectrometer. The optical absorption spectra of the samples were obtained at 298−373 K using a UV−vis spectrophotometer (Thermo Evolution 600). Elemental analyses were performed with a Perkin-Elmer 2400 series II.

**Synthesis of Compound 2.** Compound **1** (5 g, 4.7 mmol) was suspended in acetone (200 mL) containing anhydrous cesium carbonate (15.3 g, 47 mmol) and ethyl bromoacetate (3.8 mL, 23.5 mmol). The mixture was heated under nitrogen for 24 h at room temperature. After cooling to room temperature, the solid residue was removed by filtration. The residue was extracted with chloroform (100 mL × 2). The combined extracts were washed with water (80 mL × 2) and saturated brine (20 mL), dried ($MgSO_4$), and condensed under reduced pressure. The product was purified by recrystallization from hexane/dichloromethane (33.5%). $^1H$ NMR (300 MHz, $CDCl_3$): $\delta$ 1.25 (36H, s, $C(CH_3)_3$), 1.28 (12H, t, $J$ = 7.2 Hz, $CH_3$), 4.22 (8H, q, $J$ = 7.2 Hz, $COOCH_2$), 4.60 (8H, s, $OCH_2CO$), 7.51 (8H, s, ArH). ESI-MS. Calcd for $C_{56}H_{72}O_{12}S_4$: $m/z$ 1064.4, 1065.5 ($[M + 1]^+$). FT-IR: 2960 (CH), 1764 and 1736 (CO) $cm^{-1}$. Elem anal. Calcd for $C_{56}H_{72}O_{12}S_4$: C, 63.13; H, 6.81; S, 12.04. Found: C, 63.12; H, 6.72; S, 12.11.

**Synthesis of Ligand L.** The gelator **L** was prepared according to a literature procedure.[54] Compound **2** (2.0 g, 1.88 mmol) was dissolved in 150 mL of ethanol/tetrahydrofuran, and a solution of potassium hydroxide (KOH; 2.1 g, 37.5 mmol) in distilled water (3 mL) was added. The reaction mixture was stirred for 6 h at reflux. The solvent was then removed by vacuum evaporation. Then, the residue was dissolved in water and acidified with HCl. The white precipitate was collected by filtration and dried in a vacuum to yield the desired product in quantitative yield (60%). $^1H$ NMR (300 MHz, $CDCl_3$): $\delta$ 1.25 (36H, s, tBu), 4.66 (8H, s, $OCH_2$), 7.39 (8H, s, ArH). $^{13}C$ NMR (75 MHz, $CDCl_3$): $\delta$ 167.1 153.2 150.3 129.2 127.8 65.3 34.6 30.9. ESI-MS. Calcd for $C_{48}H_{56}O_{12}S_4$: $m/z$ 953.22, 975.1 ($[M + Na]^+$). FT-IR: 3421 (OH), 1695 (CO) $cm^{-1}$. Elem anal. Calcd for $C_{48}H_{56}O_{12}S_4$: C, 60.48; H, 5.92; S, 13.46. Found: C, 60.35; H, 5.72; S, 13.55.

**Preparation of $\{[Co_4Na_4(L)_3(DMF)_6(H_2O)_6]\cdot 4H_2O\}_n$ (3).** A mixture of **L** (10 mg, 0.010 mmol) and $Co(NO_3)_2\cdot 6H_2O$ (9.3 mg, 0.031 mmol) dissolved in *N*,*N*-dimethylformamide (DMF; 3 mL) was placed in a 10 mL Pyrex glass tube, and then 2−3 drops of a 0.1 M NaOH solution was added. The tube was sealed and kept at 80 °C for 24 h, followed by cooling to room temperature over 5 h. ESI-MS. Calcd for $C_{162}H_{218}Co_4N_6Na_4O_{52}S_{12}$: $m/z$ 3790.82, 3791.44 ($[M + 1]^+$). FT-IR: 3398, 2962, 1663, 1515 $cm^{-1}$. Elem anal. Calcd for $C_{162}H_{218}Co_4N_6Na_4O_{52}S_{12}$: C, 51.29; H, 5.79; N, 2.22; S, 10.14. Found: C, 51.27; H, 5.33; N, 2.26; S, 10.30.

**Preparation of $\{[Co_4K_4(L)_3(DMF)_3(H_2O)_9]\cdot 8H_2O\}_n$ (4).** A mixture of **L** (10 mg, 0.010 mmol) and $CoCl_2\cdot 6H_2O$ (7.5 mg, 0.031 mmol) dissolved in DMF (3 mL) was placed in a 10 mL Pyrex glass tube, and then 2−3 drops of a 0.1 M KOH solution was added. The tube was sealed and kept at 80 °C for 24 h, followed by cooling to room temperature over 5 h. ESI-MS. Calcd for $C_{153}H_{207}Co_4K_4N_3O_{54}S_{12}$: $m/z$ 7456.22, 7456.9 ($[M + 1]^+$). FT-IR: 3402, 2960, 2360, 1690, 1445 $cm^{-1}$. Elem anal. Calcd for $C_{153}H_{207}Co_4K_4N_3O_{54}S_{12}$: C, 49.28; H, 5.59; N, 1.13; S, 10.32. Found: C, 49.25; H, 5.49; N, 1.15; S, 10.30.

**Preparation of Metal Coordination Polymer Gels.** A solution of cobalt salt [150 $\mu$L, 1−5 equiv in $H_2O$ (0.1 M NaOH)/DMF (6:1, v/v)] was added to a solution of ligand **L** [1.0 wt % in $H_2O$ (0.1 M NaOH)/DMF (6:1, v/v)] in a vial at pH = 7.0. The metal coordination polymeric gel formed upon standing at ambient temperature. The gelation state of the material was evaluated by the criterion of "stable-to-inversion" performed in the test tube.

**Preparation of Filter Paper Test Strips.** Filter paper (10 cm × 2 cm) test strips were prepared by coating them with melted $Co(NO_3)_2$ coordination polymer gel (**G1**; 1.0 wt %) after heating followed by the removal of solvent [$H_2O$ (0.1 M NaOH)/DMF (6:1, v/v)] under a vacuum at room temperature. The gel-coated filter papers were then cut into 10 pieces (0.5 cm × 0.5 cm) to obtain the test strips, which were then used for the detection of toxic gases.

**Quantitative Detection of VGCl by a Smartphone Application.** Filter papers coated with **G1** (1.0 wt %) were exposed to $COCl_2$ gas of various concentrations (0−200 ppm) and then dried by a vacuum. The colors of the filter papers were captured by a smartphone camera. The captured images were then analyzed using the histogram of RGB within the smartphone application without any calibration.

**Detection of Toxic Analytes by UV−vis Absorption Spectroscopy.** The required analyte gases of various concentrations (0−60 ppm) were added to each strip, and ethanol was allowed to evaporate. The filter paper test strip was placed in such a way that the absorption beam falls on the spot where the toxic gas analyte was added. Absorption spectra were observed using a film sample holder.

**Scanning Electron Microscopy (SEM) Observations.** SEM micrographs of the samples were taken with a field emission scanning electron microscope (Philips XL30 S FEG). The acceleration voltage employed was 5−15 kV, and the emission current was 10 $\mu$A.

**Photophysical Studies.** UV−vis absorption spectra were determined over the range 200−800 nm and acquired both for the gel directly at room temperature and dispersed in $H_2O$ (0.1 M NaOH)/DMF (6:1, v/v). UV−vis absorption spectra of **G1** ([**L**] = 20 mM and $Co^{2+}$ (0−5 equiv)). In addition, the solid UV−vis absorption spectra of single crystals of **3** and **4** at room temperature were recorded by UV−vis spectrophotometry (using a Thermo Evolution 600 spectrophotometer).

**X-ray Crystallographic Analysis.** Crystal data for **3** and **4** were collected on a Bruker SMART APEX II ULTRA diffractometer equipped with graphite-monochromated Mo K$\alpha$ ($\lambda$ = 0.71073 Å) radiation generated by a rotating anode and a CCD detector. The cell parameters for the compounds were obtained from a least-squares refinement of the spots (from 36 collected frames). Data collection, data reduction, and semiempirical absorption correction were carried out using the software package of *APEX2*.[55] All of the calculations for the structure determination were carried out using the *SHELXTL* package.[56] In all cases, all non-hydrogen atoms were refined anisotropically and all hydrogen atoms, except those of all water molecules of **3** and **4**, were placed in calculated positions and refined isotropically in a riding manner along with their respective parent atoms. The crystals of both compounds belong to the cubic space group $I\bar{4}3d$ (No. 220) with $Z$ = 4. As the crystallographic 3-fold and 4-fold rotoinversion axes pass the cobalt atom and ligand, respectively, the asymmetric unit is composed of a 12th of the formula. Although the alkali-metal ion is situated on the 4-fold rotoinversion axis, its occupancy is adjusted to 0.33 for the charge balance. For the coordinated DMF oxygen (O4) and water oxygen (O1W) sharing the same site, the EXYZ and EADP constraints were applied in the refinement. To avoid collision between adjacent symmetry-related DMF molecules, the occupancies of the DMF molecule (O4, N1, C13, C14, and C15) and the water molecule (O1W) are fixed at 0.50. The thermal parameters of all atoms in the DMF molecule were restrained by ISOR to assist the refinement. In **4**, another coordinated water


dx.doi.org/10.1021/ic402804p | *Inorg. Chem.* 2014, 53, 3004−3011

molecule (O2W) induced a further disorder of the coordinated DMF molecule. Thus, the atoms O4, N1, C13, C14, and C15 of the DMF molecule and O2W of another water molecule have two positions with respect to each other with a site occupancy factor of 0.25. Relevant crystal collection data, refinement data for the crystal structures, and selected bond lengths and angles of **3** and **4** are summarized in Tables S1 and S2 in the Supporting Information (SI).

## RESULTS AND DISCUSSION

Tetracarboxylic acid-appended thiacalix[4]arene (**L**) containing sulfide moieties was prepared as a building block to form a network structure. There are two different metal binding sites to form the network structure. The sulfide moieties of **L** can coordinate to a soft metal ion such as $Ag^{+}$ and $Hg^{2+}$, whereas the carboxyl groups of **L** can coordinate to metal ions such as $Zn^{2+}$, $Co^{2+}$, and $Cu^{2+}$. Thus, ligand **L** forms a coordination polymeric structure with two different metal ions. This is one of the advantages compared to the classical calixarene.

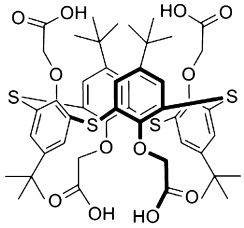

**L**

In a typical experiment, tetracarboxylic acid-appended thiacalix[4]arene (**L**) was dissolved in $H_2O$ (0.1 M NaOH) and DMF (6:1, v/v), and $Co^{2+}$ with various anions, such as $ClO_4^{-}$, $Cl^{-}$, $Br^{-}$, $I^{-}$, $SO_4^{2-}$, or $NO_3^{-}$, was dissolved in the same solvent. Strong bases, such as NaOH and KOH, dissociated the proton of ligand **L**, at which point the ligand **L** becomes anionic. The anionic type of ligand **L** easily and efficiently forms a network structure with $Co^{2+}$. The molar ratios of $Co^{2+}$ to **L** ranged from 1 to 5. **L** immediately formed a gel upon the addition of this ion in the presence of $ClO_4^{-}$, $Cl^{-}$, $Br^{-}$, $I^{-}$, $SO_4^{2-}$, or $NO_3^{-}$ counterions (Figure 1A) in $H_2O$ (0.1 M NaOH)/DMF (Table S3 and S4 in the SI) at pH = 7.0. We also tested the gel formation by changing the compositions of water and DMF. The different compositions of water/DMF (1:2, 1:4, and 1:8, v/v, and 2:1−6:1, v/v) did not form the coordination polymer gel (Table S4 in the SI). Except for the gel containing $Cl^{-}$, these gels were purple (Figure 1A). In a field-emission SEM image of the $Co(NO_3)_2$ coordination polymer gel (**G1**), spherical structures were seen as 20−30-nm-diameter particles (Figure 1B). In addition, SEM images of the coordination polymer gels obtained using different anions also showed similar spherical particles (Figure S1 in the SI). These findings thus suggest that the morphology of the $Co^{2+}$ coordination polymer gel does not strongly depend on the nature of the anion. The UV−vis absorption spectra of the $Co(NO_3)_2$ coordination polymer gel (**G1**) and the $CoCl_2$ coordination polymer gel (**G2**) were obtained (Figure S2 in the SI).

The absorption of red **G1** displayed a maximum at 527 nm (Figure S2A in the SI), indicative of the octahedral structure.[57] In contrast, the absorption band of blue **G2** was very broad, with a maximum at 670 nm (Figure S2B in the SI). According to the curve-fitting method, the broadened absorption band for **G2** consisted of two components corresponding to ∼3:1 relative concentration for the bands at 527 and 670 nm. Hence, the differences in color between **G1** and **G2** are due to differences in the coordination geometry.

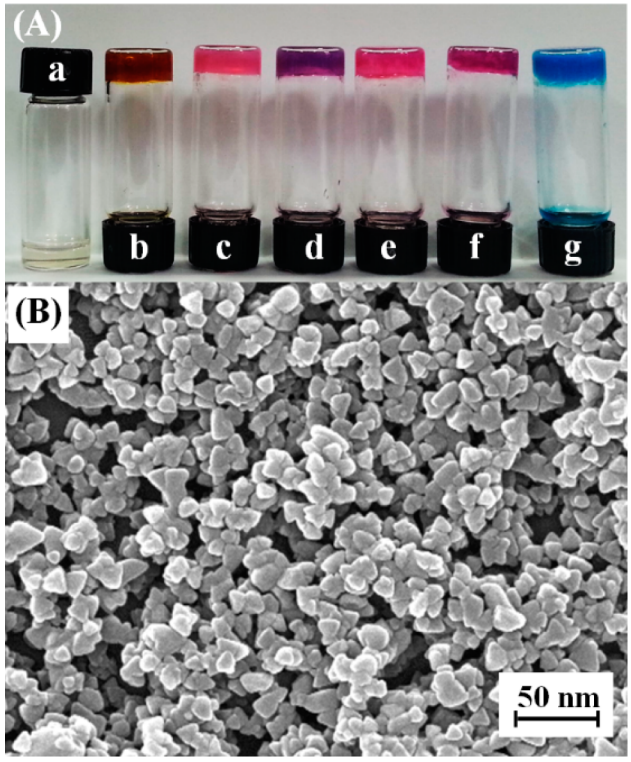


**Figure 1.** (A) Photographs of the coordination polymer gels (**L**: 1.0 wt %) without (a) metal ion and with (b) $CoI_2$, (c) $Co(NO_3)_2$, (d) $CoBr_2$, (e) $Co(ClO_4)_2$, (f) $CoSO_4$, and (g) $CoCl_2$ in $H_2O$ (0.1 M NaOH)/DMF (6/1, v/v) at pH = 7.0. A total of 3.0 equiv of $Co^{2+}$ was added to a **L** solution (1.0 wt %). (B) SEM image of the coordination polymer gel (1.0 wt %) with $Co(NO_3)_2$ (3 equiv) at pH = 7.0.

To further elucidate the driving forces for gel formation as well as the relationship between the differences in the color and geometry of **G1** and **G2**, we attempted to grow both the red and blue high-quality single crystals of $Co^{2+}$ complexes of **L** from the gel phase. However, the quality of both the red and blue single crystals was too poor for X-ray crystallographic analysis. Between the molecular assembled structures in the gel phase are generally quite similar to those of the single-crystal structures obtained from solution,[58−60] the relationship between the color and geometry of **G1** and **G2** was investigated by X-ray crystallographic analysis of single crystals grown in DMF. Single crystals of both the red and blue forms were investigated by X-ray crystallographic analysis. When the solvothermal reactions of $H_4$**L** with cobalt salts ($NO_3^{-}$ for **3** and $Cl^{-}$ for **4**) were carried out, no solid product was obtained. However, treatment of this reaction mixture with a small amount of NaOH for **3** or KOH for **4** afforded two kinds of crystalline products: a purple compound of type $\{[Co_4Na_4(\mathbf{L})_3(DMF)_6(H_2O)_6]\cdot 4H_2O\}_n$ (**3**) and a blue compound of type $\{[Co_4K_4(\mathbf{L})_3(DMF)_3(H_2O)_9]\cdot 8H_2O\}_n$ (**4**). X-ray analysis revealed that both **3** and **4** are isostructures differing only by the coordination environment around the cobalt(II) ion and the type of alkali-metal ion present; their asymmetric units contain a 12th of the formula unit. The X-ray crystal structures of both compounds are shown in Figure 2, with selected geometric parameters listed in Tables S1 and S2 in the SI.


dx.doi.org/10.1021/ic402804p | Inorg. Chem. 2014, 53, 3004−3011

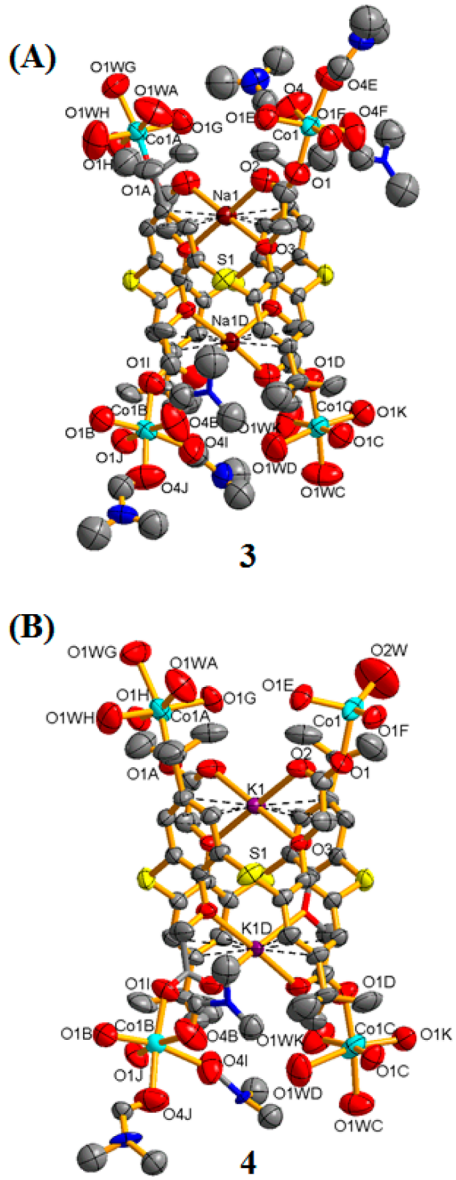


**Figure 2.** Single-crystal structures of (A) **3** and (B) **4** with views of the $Co^{2+}$ coordination environments.

In both crystal structures, $L^{4-}$ adopts the 1,3-alternative conformation and accommodates the alkali-metal ions ($Na^+$ for **3** and $K^+$ for **4**) with an abundance ratio of 1.33 per one $L^{4-}$ inside the calix cavity. Each alkali-metal atom displays a distorted square-planar geometry of two monodentate carboxylate oxygen atoms and two phenolic oxygen atoms from two different 1,3-alternate pendant groups in a cis arrangement [O−M−O = 62.5(2)−120.8(3)° for **3** and 60.68(12)−120.55(16)° for **4**]. The alkali-metal atom also interacts with the aromatic rings via $\eta^3$-type cation···$\pi$ interactions[61−63] [dashed lines in Figure 2; 3.459(8)−3.467(8) Å for **3** and 3.411(6)−3.458(6) Å for **4**]. One $L^{4-}$ ligand is coordinated to four crystallographically equivalent cobalt(II) ions. However, each cobalt(II) center has a different coordination environment because of the different arrangements of solvent molecules ($H_2O$ and DMF) in the respective coordination shells. In the red complex **3**, the four cobalt(II) atoms each adopt a distorted octahedral geometry, but two of them are coordinated by three carboxylate oxygen atoms from three different $L^{4-}$ ligands in a monodentate manner and also by three water molecules. The other two cobalt(II) atoms are bound by three monodentate carboxylate oxygen atoms from three different $L^{4-}$ ligands and three DMF oxygen atoms (Figure 2A).

In the blue complex **4**, three of the four cobalt(II) atoms are bound to three monodentate carboxylate oxygen atoms from three different molecules of $L^{4-}$ and to three water or three DMF molecules to form distorted octahedral environments, similar to those in **3**. However, very interestingly, the fourth cobalt(II) atom adopts a distorted tetrahedral geometry, being bound to three carboxylate oxygen atoms from three different $L^{4-}$ in a monodentate manner. The coordination sphere of this metal center is completed by a water molecule (Figure 2B). Importantly, the presence of the cobalt(II) atom with tetrahedral geometry clearly distinguishes **4** from **3** and is very likely the cause of the observed change in color from red for **3** to blue for **4**. One $L^{4-}$ ligand is linked to four different cobalt(II) atoms connected to three different $L^{4-}$ ligands via Co−O(carboxylate) coordination bonds in a monodentate manner to afford the 3D motif (Figure S3 in the SI). The powder XRD patterns of the single crystals **3** and **4** are also compared to those for **G1** and **G2** (Figure S4 in the SI). The powder XRD pattern ranging from $\theta$ = 13 to 50° in single crystal **3** is different from that of single crystal **4** (Figure S4C in the SI). The pattern at the [211] face obtained from **G1**, **G2**, and red and blue crystals **3** and **4** was the highest, indicating that these gels and crystals may be oriented into the [211] face. Furthermore, the bonding lengths of both the [211] and [220] faces of **G1** are the same as those of the red crsytal **3**. Among the four materials, the pattern at the [211] face obtained from the blue crsytal **4** was the highest, indicating that the blue crystal **4** may be well oriented into the [211] face. On the other hand, the powder XRD patterns of the red and blue single crystals of $Co^{2+}$ complexes are quite similar to those obtained for **G1** and **G2**, indicating that the single-crystal structures of $Co^{2+}$ complexes are similar to those of **G1** and **G2**.

To probe the mechanism of the change from an octahedral structure to a tetrahedral structure of $Co^{2+}$, the introduction of $COCl_2$ gas to a red single crystal of the $Co^{2+}$ complex was performed. The red single crystal changed to a blue-colored powder. The powder XRD pattern of the blue-colored powders obtained with $COCl_2$ gas was also compared to that of the original blue single crystal of the $Co^{2+}$ complex (Figure S5 in the SI). The powder XRD pattern of the blue powders of single crystal **3** after diffusion of $COCl_2$ gas is similar to that of the blue single crystal **4**. This is clear evidence for the coordination geometry of single crystal **4**, in which one of the octahedral structure was changed into the tetrahedral structure. In addition, elemental compositions of the blue powder obtained by the introduction of $COCl_2$ gas were analyzed by SEM with EDX equipment (Figure S6 in the SI). The EDX spectrum of the blue powder of $Co^{2+}$ shows carbon, nitrogen, sulfur, sodium, and cobalt components. These studies clearly indicated that conversion of the red crystal with the octahedral structure into a blue color upon the introduction of $COCl_2$ gas was due to the removal of three DMF molecules presumably by an intermolecular hydrogen-bonding interaction between DMF and HCl. In addition, elemental analysis and ICP of the blue-colored powders obtained with $COCl_2$ gas demonstrated an elemental content profile of 52.33% for C, 5.35% for H, 1.08% for N, 10.95% for S, 2.55% for Na, and 6.63% for $Co^{2+}$. These results are in excellent agreement with the calculated data: C,


dx.doi.org/10.1021/ic402804p | Inorg. Chem. 2014, 53, 3004−3011

52.20%; H, 5.47%; N, 1.19%; S, 10.93%; O, 20.90%; Na, 2.61%; $Co^{2+}$, 6.70%. Therefore, the geometric change of a thiacalix[4]-arene supramolecular gel with VGCl in this work would occur by the following steps. In the step 1, $Co^{2+}$ forms the octahedral structure, having three DMF and three water molecules. In the first step, which involves octahedral cobalt gels, the aqueous pH condition is adjusted to neutral (pH = 7.0). In the step 2, $COCl_2$ gas is hydrolyzed to HCl in the presence of $H_2O$. Then, HCl molecules remove three DMF molecules in the $Co^{2+}$ complex by forming an intermolecular hydrogen-bonding interaction, turning to the tetrahedral structure in the step 3. Once again, HCl produced by hydrolysis of $COCl_2$ (eq 2) forms an intermolecular hydrogen-bonding interaction with DMF molecules. It is known that the oxygen atom of DMF interacts with the hydrogen atom of HCl.[64] Therefore, the HCl molecule cleaves the bond between $Co^{2+}$ and DMF because the coordination bond between $Co^{2+}$ and DMF is comparatively weaker than the intermolecular hydrogen bond between HCl and DMF.

$$3\mathbf{L} + 4Co(NO_3)_2 \rightarrow \{[Co_4Na_4(\mathbf{L})_3(DMF)_6(H_2O)_6]\cdot 4H_2O\}_n \quad (1)$$

$$3COCl_2 + 9H_2O \rightarrow 3CO_2 + 6HCl + 6H_2O \quad (2)$$

$$2[Co_4Na_4(\mathbf{L})_3(DMF)_6(H_2O)_6]_n + 6HCl + 6H_2O \rightarrow 2[Co_4Na_4(\mathbf{L})_3(DMF)_3(H_2O)_9]_n + 6(DMF\cdot HCl) \quad (3)$$

We also acquired the UV−vis absorption spectra of single crystals **3** and **4** by a curve-fitting method (Figure 3). As with

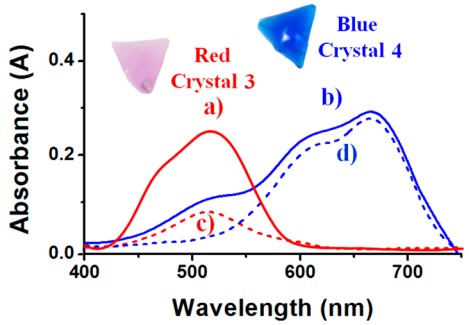


**Figure 3.** Solid UV−vis absorption spectra of red crystal **3** (a: red curve) and blue crystal **4** (b: blue curve). (c and d) Absorption spectra obtained from part b by a curve-fitting method.

**G1** and **G2**, the absorption of a single red crystal of **3** exhibited a maximum at 527 nm (Figure 3, curve a). On the other hand, a single blue crystal of **4** exhibited a very broad absorption with a maximum at 670 nm (Figure 3, curve b). The broadened absorption band of the blue single crystal was separated by the curve-fitting method to reveal two distinct absorption bands at 527 and 670 nm (Figure 3, curves c and d). We calculated the contributions of the two species to the spectrum and determined that the octahedral and tetrahedral structures consist of ~3:1 relative concentration. Although the contribution of the tetrahedral structure to the geometric ratio is lower than that of the octahedral structure, the blue color of a single crystal is dominated with the tetrahedral structure because of its relatively higher extinction coefficient. The result is in good agreement with a single crystallographic result.

Toxic gases can contaminate the human body, clothing, and other materials in the surroundings during manufacturing. For example, phosgene ($COCl_2$) was used as a chemical weapon during World War I.[65] The largest users of toxic organic or inorganic compounds containing chlorine atoms are companies that make ethylene dichloride and other chlorinated solvents, poly(vinyl chloride) resins, chlorofluorocarbons, and propylene oxide.[66] Paper companies use chlorine to bleach paper. In addition to its industrial production, small amounts of chlorine occur naturally from the breakdown and combustion of VGCl, such as those used in refrigeration systems.[67] In such cases, the contact mode is the appropriate means to check for residual contamination by vaporized chemical or toxic gas. As a result, a convenient detection method for vaporized chlorinated compounds is potentially of considerable importance to the environmental and biological fields.[68,69]

To investigate the application of the present gels as chemoprobes for VGCl, we prepared test strips by transferring gel nanoparticles onto a Whatman filter paper (No. 42) by dipping the paper into a hot solution of the gel, followed by drying under a vacuum and cutting of the dried filter paper into sections. Then, the **G1**-coated filter paper was inspected by SEM. As shown in Figure S7 in the SI, the SEM image shows that the paper was covered by spherical nanoparticles (20−30 nm), with ca. 4 $\mu$m thickness. The particles were similar in appearance to **G1** itself. The filter paper strips were then tested as chemoprobes for phosgene ($COCl_2$) gas. The **G1**-coated filter paper was placed in a vial containing phosgene gas at room temperature. The absorption spectra were measured using a front-face technique after exposure to the test strip for 10 s (Figure 4A).

A significant absorbance change was observed (Figure 4A,B) upon exposure to $COCl_2$ gas for 10 s. The red **G1**-coated filter paper changed to blue. The absorption band at 527 nm gradually decreased, and with prolonged exposure for 60 s to

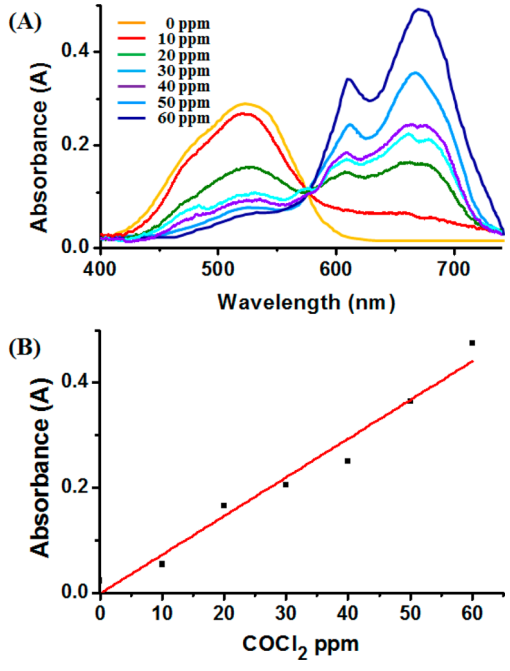


**Figure 4.** (A) Solid UV−vis absorption spectra of filter papers coated with **G1** after diffusion of $COCl_2$ (0−60 ppm). (B) Plot of absorbance at 670 nm against the concentration of $COCl_2$.


dx.doi.org/10.1021/ic402804p | Inorg. Chem. 2014, 53, 3004−3011

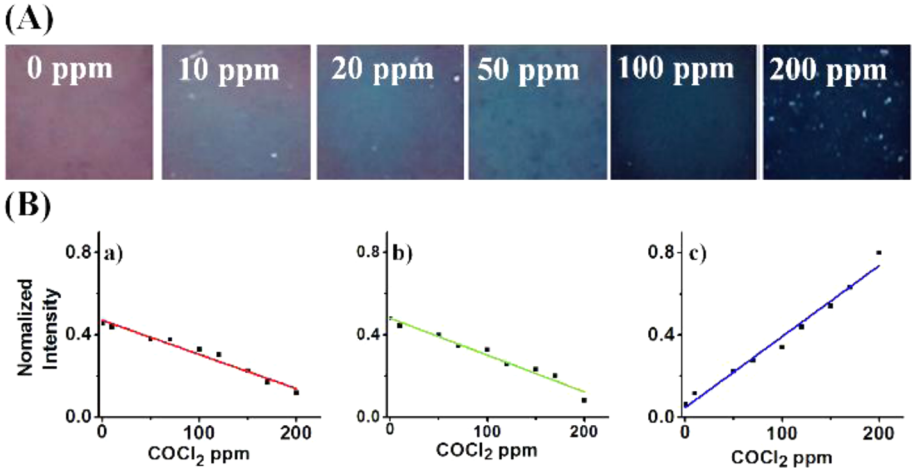


**Figure 5.** (A) Photographs of filter papers coated with **G1** after diffusion of $COCl_2$ gas (0−200 ppm). (B) Plots of $COCl_2$ against RGB intensities obtained by a smartphone: (a) red, (b) green, and (c) blue colors.

$COCl_2$ gas, the absorbance at 670 nm gradually increased (Figure S8 in the SI). The findings indicate that the octahedral structure of **G1**-coated filter paper is partially changed to the tetrahedral structure. Absorption changes were observed over the range 10−200 ppm ($COCl_2$) with good linearity and with a rapid response of several seconds. In addition, the response of the filter paper to $COCl_2$ gas exhibited good reproducibility over several repeated measurements under the same conditions. The introduction of HCl, $SOCl_2$, and $COCl_2$ gases to **G1**-coated filter paper also induced a similar red-to-blue color change (Figure S9 in the SI). On the other hand, no significant color changes were observed when the test strips were exposed to HF, HBr, HI, and $HNO_3$ (Figure S10 in the SI). These findings indicate that **G1**-coated filter paper is useful as a chemoprobe and adsorbent for VGCl.

As a reference experiment, when **G1** was added to NaCl in water, there was no no significant change in the red color of **G1** (Figure S11 in the SI) because $Cl^-$ does not coordinate to $Co^{2+}$. In this system, $H_2O$ and DMF molecules act as stronger ligands compared to $Cl^-$. In addition, we observed the red color change of **G1** upon the addition of NaCl in methanol. There was no change in the red color of **G1**. The results indicate that $Cl^-$ does not coordinate to $Co^{2+}$. There are several reasons for the selective color change of **G1** with VGCl. The selective color changes of **G1** upon the addition of VGCl would relate to the strength of the intermolecular hydrogen bonds and electronegativity of the halide atoms. HF, HBr, and $HNO_3$ moelcules can also interact with DMF. However, the strengths of the intermolecular hydrogen bonds between HBr or $HNO_3$ and DMF are weaker than that of the coordination bond between $Co^{2+}$ and DMF. In the case of HF, HF is easily ionized in high-humidity conditions compared with other gases. Thus, VGCl molecules induce the selective color change from red to blue.

Recently, digital cameras integrated in portable devices such as tablets and smartphones have been applied as image detectors because the built-in microprocessors can be programmed to carry out the image processing necessary to determine an analyte concentration.[70−73] In addition, there are several advantages in a smartphone as a color reader. First, a smartphone is very easily portable in any place. Second, a smartphone is cheaper than a UV−vis absorption spectrometer. Moreover, applications for open systems such as Android and iPhone operating system (iOS) can be easily programmed and implemented on many smart devices. The response of the filter paper coated with **G1** test strips was evaluated over the range of 10−200 ppm of $COCl_2$ gas at room temperature (Figure 5A). First, the red filter paper was exposed to a constant concentration of $COCl_2$ gas for 10 s at room temperature, during which the red color progressively changed to blue (Figure 5A). Second, the images of the filter paper exposed to $COCl_2$ gas were captured by a smartphone camera. The captured images were analyzed using the histogram of RGB via the smartphone application without any calibration. The calibration curves are shown in Figure 5B. The curves obtained from RGB show excellent linearity with a correlation coefficient ($r^2$) of 0.995−0.999. Among the three calibration curves obtained, the curve obtained for blue gave the best correlation coefficient with 0.999. The limit of detection using the curve for blue was 2.5 ppm. Moreover, the time required to predict the VGCl concentration from the image is much shorter using the smartphone compared to using an expensive and cumbersome spectrophotometer and, hence, the use of a smartphone with a high-resolution camera as an image detector provides a great advantage.

## ■ CONCLUSIONS

We have demonstrated a rare example of a selective chemoprobe for the detection of VGCl with interconversion between structures in the gel state. A thiacalix[4]arene-based ligand efficiently produces a coordination polymer gel by simple mixing with a $Co^{2+}$ ion. The octahedral and mixed octahedral−tetrahedral structures of the single crystals of the present $Co^{2+}$ complexes were clearly confirmed by single-crystal X-ray analysis. More interestingly, the red color of filter paper coated with **G1** with the octahedral structure was selectively changed to a blue color by exposure to toxic VGCl such as HCl, $SOCl_2$, $(COCl)_2$, and $COCl_2$ that hydrolyze to yield HCl. The color change was due to a change in the coordination geometry from octahedral to tetrahedral with at least one cobalt(II) center, which is an example of gasochromism. The geometric change of **G1** from an octahedral structure to a tetrahedral structure upon the introduction of phosgene gas has been indirectly demonstrated by the single-crystal X-ray studies of $Co^{2+}$ complexes. The red color change of **G1** with octahedral structures into the blue color by the introduction of VGCl appears to be due to the removal of three DMF molecules by


dx.doi.org/10.1021/ic402804p | Inorg. Chem. 2014, 53, 3004−3011

the intermolecular hydrogen-bonding interaction between DMF and HCl to form the tetrahedral structure. Furthermore, the camera in particular smartphones is capable of detecting VGCl by use of the histogram of RGB within the Android and iOS application. The present study is a rare example of the application of a coordination polymer gel as a chemoprobe for VGCl such as HCl, $SOCl_2$, $(COCl)_2$, and $COCl_2$. These results suggest that the filter paper coated with **G1** may also lead to useful applications in other vaporized chemical sensing applications. The concepts employed in the present study should open the door for a range of new sensors based on responsive soft materials such as **G1** described here.

## ■ ASSOCIATED CONTENT

### Ⓢ Supporting Information

X-ray crystallographic data of **3** and **4** in CIF format, information on the gelation test, and spectroscopic data. This material is available free of charge via the Internet at http://pubs.acs.org.

## ■ AUTHOR INFORMATION


### Corresponding Author

*E-mail: jonghwa@gnu.ac.kr. Fax: +82-55-758-6027.


### Notes

The authors declare no competing financial interest.

## ■ ACKNOWLEDGMENTS

This work was supported by a grant from the NRF (Grant 2012002547) supported by the Ministry of Education, Science and Technology, Korea. In addition, this work was partially supported by a grant from the Next-Generation BioGreen 21 Program (SSAC, Grant PJ009041), Rural Development Administration, Korea.

## ■ REFERENCES


(1) Fages, F. *Angew. Chem., Int. Ed.* **2006**, *45*, 1680.
(2) Leong, W. L.; Tam, A. Y.-Y.; Batabyal, S. K.; Koh, L. W.; Kasapis, S.; Yam, V. W.-W.; Vittal, J. J. *Chem. Commun.* **2008**, 3628.
(3) Batabyal, S. K.; Leong, W. L.; Vittal, J. J. *Langmuir* **2010**, *26*, 7464.
(4) Leong, W. L.; Batabyal, S. K.; Kasapis, S.; Vittal, J. J. *Chem.—Eur. J.* **2008**, *14*, 8822.
(5) Paulusse, J. M. J.; van Beek, D. J. M.; Sijbesma, R. P. *J. Am. Chem. Soc.* **2007**, *129*, 2392.
(6) Hui, J. K.-H.; Yu, Z.; MacLachlan, M. J. *Angew. Chem., Int. Ed.* **2007**, *46*, 7980.
(7) Weng, W.; Beck, J. B.; Jamieson, A. M.; Rowan, S. J. *J. Am. Chem. Soc.* **2006**, *128*, 11663.
(8) Kim, H.-J.; Lee, J.-H.; Lee, M. **2005**, *44*, 5810.
(9) Lloyd, G. O.; Steed, J. W. *Nat. Chem.* **2009**, *1*, 437.
(10) Jung, J. H.; Lee, J.; Siverman, J. R.; John, G. *Chem. Soc. Rev.* **2013**, *42*, 924.
(11) Kartha, K. K.; Babu, S. S.; Srinivasan, S.; Ajayaghosh, A. *J. Am. Chem. Soc.* **2012**, *134*, 4834.
(12) Sajisha, V. S.; Maitra, U. *Chemia* **2013**, *67*, 44.
(13) Lee, H.; Kang, S.; Lee, J. Y.; Jung, J. H. *Soft Matter* **2012**, *8*, 2950.
(14) Roubeau, O.; Colin, A.; Schmitt, V.; Clerac, R. *Angew. Chem., Int. Ed.* **2004**, *43*, 3283.
(15) Shirakawa, M.; Fujita, N.; Tani, T.; Kaneko, K.; Ojima, M.; Fujii, A.; Ozaki, M.; Shinkai, S. *Chem.—Eur. J.* **2007**, *13*, 4155.
(16) Piepenbrock, M.-O.; Clarke, N.; Steed, J. W. *Langmuir* **2009**, *25*, 8451.
(17) Babu, S. S.; Praveen, V. K.; Prasanthkumar, S.; Ajayaghosh, A. *Chem.—Eur. J.* **2008**, *14*, 9577.
(18) Babu, S. S.; Kartha, K. K.; Ajayaghosh, A. J. *Phys. Chem. Lett.* **2010**, *1*, 3413.
(19) Kuroiwa, K.; Shibata, T.; Takada, A.; Nemoto, N.; Kimizuka, N. *J. Am. Chem. Soc.* **2004**, *126*, 2016.
(20) Lee, H.; Jung, S. H.; Han, W. S.; Moon, J. H.; Kang, S.; Lee, J. Y.; Jung, J. H.; Shinkai, S. *Chem.—Eur. J.* **2011**, *17*, 2823.
(21) Yen, C.-W.; Chen, J.-D. *Inorg. Chem. Commun.* **2011**, *14*, 1212.
(22) Morris, P. J.; Martin, R. B. *J. Am. Chem. Soc.* **1970**, *92*, 1543.
(23) Fu, S.-J.; Cheng, C.-Y.; Lin, K.-J. *Cryst. Growth Des.* **2007**, *7*, 1381.
(24) Wu, H.; Liu, B.; Kou, F.; Jia, F.; Yuan, J.; Bai, Y. *Z. Anorg. Allg. Chem.* **2012**, *638*, 122.
(25) Borah, M. J.; Singh, R. K. B.; Sinha, U. B.; Swu, T.; Borah, P. J. *J. Chem. Crystallogr.* **2012**, *42*, 67.
(26) Perkins, D. F.; Lindoy, L. F.; McAuley, A.; Meehan, G. V.; Turner, P. *Proc. Natl. Acad. Sci. U. S. A.* **2006**, *103*, 532.
(27) Atkinson, I. M.; Lindoy, L. F. *Coord. Chem. Rev.* **2000**, *200*, 207.
(28) Ikeda, A.; Shinkai, S. *Chem. Rev.* **1997**, *97*, 1713.
(29) Mecca, T.; Messina, G. M. L.; Marletta, G.; Consolo, F. *Chem. Commun.* **2013**, *49*, 2530.
(30) Aoki, M.; Nakashima, K.; Kawabata, H.; Tsutsui, S.; Shinkai, S. *J. Chem. Soc., Perkin Trans. 2* **1993**, 347.
(31) Aoki, M.; Murata, K.; Shinkai, S. *Chem. Lett.* **1991**, 1715.
(32) Kim, K.; Park, S.; Park, K.-M.; Lee, S. S. *Cryst. Growth Des.* **2011**, *11*, 4059.
(33) Cai, X.; Wu, Y.; Wang, L.; Yan, N.; Liu, J.; Fang, X.; Fang, Y. *Soft Matter* **2013**, 5807.
(34) Bew, S. P.; Burrows, A. D.; Duren, T.; Mahon, M. F.; Moghadam, P. Z.; Sebestyen, V. M.; Thurston, S. *Chem. Commun.* **2012**, *48*, 4824.
(35) Yamada, M.; Ootashiro, Y.; Kondo, Y.; Hamada, F. *Tetrahedron Lett.* **2013**, *54*, 1510.
(36) Messina, M. T.; Metrangolo, P.; Pappalardo, S.; Parisi, M. F.; Pilati, T.; Resnati, G. *Chem.—Eur. J.* **2000**, *6*, 3495.
(37) Kim, S. K.; Lynch, V. M.; Young, N. J.; Hay, P. B.; Lee, C.-H.; Kim, J. S.; Moyer, B. A.; Sessler, J. L. *J. Am. Chem. Soc.* **2012**, *134*, 20837.
(38) Nakamura, R.; Ikeda, A.; Sarson, L. D.; Shinkai, S. *Supramol. Chem.* **1998**, *9*, 25.
(39) Ikeda, A.; Irisa, T.; Hamano, T.; Kitahashi, T.; Sasaki, Y.; Hashizume, M.; Kikuchi, J.; Konishi, T.; Shinkai, S. *Org. Biomol. Chem.* **2006**, *4*, 519.
(40) Xing, B.; Choi, M.-F.; Xu, B. *Chem.—Eur. J.* **2002**, *8*, 5028.
(41) Goh, C. Y.; Becker, T.; Brwon, D. H.; Skelton, B. W.; Jones, F.; Mocerino, M.; Ogden, M. I. *Chem. Commun.* **2011**, *47*, 6057.
(42) Becker, T.; Goh, C. Y.; Jones, F.; McIldowie, M. J.; Mocerino, M.; Ogden, M. I. *Chem. Commun.* **2008**, 3900.
(43) Zhang, J.; Guo, D.-S.; Wang, L.-H.; Wang, Z.; Liu, Y. *Soft Matter* **2011**, *7*, 1756.
(44) Harrowfield, J.; Koutsantonis, G. Calixarenes as Cluster Keeper. In *Calixarenes in the Nanoworld*; Vicens, J., Harrowfield, J., Eds.; Springer: Dordrecht, The Netherlands, 2007; p 197.
(45) Morohashi, N.; Narumi, F.; Iki, N.; Hattori, T.; Miyano, S. *Chem. Rev.* **2006**, *106*, 5291.
(46) Kajiwara, T.; Iki, N.; Yamashita, M. *Coord. Chem. Rev.* **2007**, *251*, 1734.
(47) Macias, A. T.; Norton, J. E.; Evanseck, J. D. *J. Am. Chem. Soc.* **2003**, *125*, 2351.
(48) Praveen, L.; Ganga, V. B.; Thirumalai, R.; Sreeja, T.; Reddy, M. L. P.; Luxmi Varma, R. *Inorg. Chem.* **2007**, *46*, 6277.
(49) Chen, T.; Chen, Q.; Zhang, X.; Wang, D.; Wan, L.-J. *J. Am. Chem. Soc.* **2010**, *132*, 5598.
(50) Dai, F.-R.; Wang, Z. *J. Am. Chem. Soc.* **2012**, *134*, 8002.
(51) Liu, M.; Liao, W.; Hu, C.; Du, S.; Zhang, H. *Angew. Chem., Int. Ed.* **2012**, *51*, 1585.
(52) Kumar, M.; Dhir, A.; Bhalla, V. *Org. Lett.* **2009**, *11*, 2567.
(53) Kumar, M.; Kumar, R.; Bhalla, V. *Chem. Commun.* **2009**, 7384.
(54) Iki, N.; Morohashi, N.; Narumi, F.; Fujimoto, T.; Suzuki, T.; Miyano, S. *Tetrahedron Lett.* **1999**, *40*, 7337.

(55) *APEX 2 Version 2009.1-0 Data Collection and Processing Software*; Bruker AXS Inc.: Madison, WI, 2008.
(56) A Short History of *SHELX*: Sheldrick, G. M. *Acta Crystallogr.* **2008**, *A64*, 112.
(57) Miessler, G. L.; Tarr, D. A. *Inorganic Chemistry*; 3rd ed.; Prentice Hall: Upper Saddle River, NJ, 2004.
(58) Anderson, K. M.; Day, G. M.; Paterson, M. J.; Byrne, P.; Clarke, N.; Steed, J. W. *Angew. Chem., Int. Ed.* **2008**, *47*, 1058.
(59) Adarsh, N. N.; Dastidar, P. *Cryst. Growth Des.* **2011**, *11*, 328.
(60) Trivedi, D. R.; Dastidar, P. *Chem. Mater.* **2006**, *18*, 1470.
(61) Liu, Y.-J.; Huang, J.-S.; Chui, S. S.-Y.; Li, C.-H.; Zuo, J.-L.; Zhu, N.; Che, C.-M. *Inorg. Chem.* **2008**, *47*, 11514.
(62) Zheng, X.; Wang, X.; Shen, K.; Wang, N.; Peng, Y. *J. Comput. Chem.* **2010**, *31*, 2143.
(63) Zeller, J.; Radius, U. *Inorg. Chem.* **2006**, *45*, 9487.
(64) Kislina, I. S.; Librovich, N. B.; Maiorov, V. D. *Russ. Chem. Bull.* **1994**, *43*, 1505.
(65) Bly, R. S.; Perkins, G. A.; Lewis, W. *J. Am. Chem. Soc.* **1922**, *44*, 2896.
(66) Stringer, R.; Johnston, P. *Chlorine and the Environment: An Overview of the Chlorine Industry*; Kluwer Academic: Dordrecht, The Netherlands, 2001; p 25.
(67) Intergovernmental Panel on Climate Change/Technology and Economic Assessment Panel (IPCC/TEAP). *IPCC/TEAP Special Report on Safeguarding the Ozone Layer and the Global Climate System: Issues Related to Hydrofluorocarbons and Perfluorocarbons*; Cambridge University Press: Cambridge, U.K., 2005.
(68) Chen, C.; Campbell, K. D.; Negi, I.; Iglesias, R. A.; Owens, P.; Tao, N.; Tsow, F.; Forzani, E. S. *Atmos. Environ.* **2012**, *54*, 679.
(69) Hierlemann, A.; Weimar, U.; Kraus, G.; Schweizer-Berberich, M.; Gopel, W. *Sens. Actuators B* **1995**, *26*, 126.
(70) Lopez-Ruiz, N.; Martinez-Olmos, A.; Perez de Vargas-Sansalvador, I. M.; Fernandez-Ramos, M. D.; Carvajal, M. A.; Capitan-Vallvey, L. F.; Palma, A. J. *Sens. Actuators B* **2012**, *171−172*, 938.
(71) Haun, J. B.; Castro, C. M.; Wang, R.; Peterson, V. M.; Marinelli, B. S.; Lee, H.; Weissleder, R. *Sci. Transl. Med.* **2011**, *3*, 7116.
(72) Wei, Q.; Qi, H.; Luo, W.; Tseng, D.; Ki, S. J.; Wan, Z.; Gorocs, Z.; Bentolila, L. A.; Wu, T.-T.; Sun, R.; Ozcan, A. *ACS Nano* **2013**, *7*, 9147.
(73) Khatua, S.; Orrit, M. *ACS Nano* **2013**, *7*, 8340.